

Enhanced critical parameters of nanocarbon doped MgB₂ superconductorMonika Mudgel,^{1,3} L. S. Sharath Chandra,² V. Ganesan,² G. L. Bhalla,³ H. Kishan,¹ and V. P. S. Awana^{1,a)}¹National Physical Laboratory, Dr. K. S. Krishnan Road, New Delhi 110012, India²UGC-DAE Consortium for Scientific Research, University Campus, Khandwa Road, Indore 452017, India³Department of Physics and Astrophysics, University of Delhi, New Delhi 110007, India

(Received 29 April 2009; accepted 26 June 2009; published online 4 August 2009)

The high field magnetization and magnetotransport measurements are carried out to determine the critical superconducting parameters of MgB_{2-x}C_x system. The synthesized samples are pure phase and the lattice parameter evaluation is carried out using the Rietveld refinement. The $R-T(H)$ measurements are done up to a field of 140 kOe. The upper critical field values, H_{c2} , are obtained from these data based on the criterion of 90% of normal resistivity, i.e., $H_{c2}=H$ at which $\rho = 90\% \rho_N$, where ρ_N is the normal resistivity, i.e., resistivity of about 40K in our case. The Werthamer–Helfand–Hohenberg prediction of $H_{c2}(0)$ underestimates the critical field value even below the field up to which measurement is carried out. After this model, the Ginzburg–Landau theory is applied to the $R-T(H)$ data which not only calculate the $H_{c2}(0)$ value but also determine the dependence of H_{c2} on temperature in the low temperature high field region. The estimated $H_{c2}(0)=157.2$ kOe for pure MgB₂ is profoundly enhanced to 297.5 kOe for the $x=0.15$ sample in MgB_{2-x}C_x series. Magnetization measurements are done up to 120 kOe at different temperatures and the other parameters such as irreversibility field H_{irr} and critical current density $J_c(H)$ are also calculated. The nano carbon doping results in substantial enhancement of critical parameters such as H_{c2} , H_{irr} , and $J_c(H)$ in comparison to the pure MgB₂ sample. © 2009 American Institute of Physics. [DOI: 10.1063/1.3186048]

I. INTRODUCTION

In the early years of discovery of renowned MgB₂ superconductor, it attracted the huge interest of scientific community due to its simple chemical composition, crystal structure, and highest T_c among the intermetallic noncuprate compounds.¹⁻³ The compound was studied extensively both by experimental and theoretical aspects by various groups. Soon, the typical and peculiar properties of MgB₂ came into picture like the two band nature having double band gap and the unusual Fermi surface topology.^{4,5} Various groups studied the band structure unfolding the mystery of different nature of Fermi surfaces for different^{3,4,6,7} bands. MgB₂ has two bands, namely, σ and π . The Fermi surface due to σ band has cylindrical sheets while possessing tubular networks is due to π band. After all these studies on structural, electronic, and band related properties of MgB₂,⁶⁻⁹ the next step is to determine the effect of this two band nature on the critical properties of MgB₂ to estimate its practical value. The effect of two band nature on critical parameters such as the upper critical field, H_{c2} , is needed to be probed. The H_{c2} increases linearly near T_c with decreasing temperature but its behavior changes in the low temperature high field region. A sharp jump is predicted by theoretical and experimental reports near $T=0$ K in the H_{c2} versus T line.¹⁰⁻¹² That is why the exact $H_{c2}(0)$ value is much higher than it seems to be through normal extrapolation of data. The Werthamer–Helfand–Hohenberg (WHH) formula determines $H_{c2}(0)$

value based on the slope of H_{c2} versus T line at $T=T_c$. But since the slope is varying with the temperature considerably, it results in the wrong estimation of H_{c2} . After that Ginzburg–Landau (GL) theory is used for the calculation of $H_{c2}(0)$. The experimental data fit very well with the GL equation and the value of $H_{c2}(0)$ is found to be much higher than the WHH formula.

The critical properties of MgB₂ can be enhanced by *nanoparticle* doping.¹³⁻¹⁵ Thus, along with MgB₂, the nanocarbon doped samples are also taken into consideration. The critical parameters such as H_{c2} , H_{irr} , and J_c enhance significantly by nanocarbon substitution at boron site. The values of critical parameters obtained are either competitive or superior than those obtained earlier. The critical current density, J_c , increases by more than an order with nanocarbon doping as estimated from magnetization plots. The substitution at boron site is more effective than nanoparticle additions in MgB₂ matrix. That is why the present results are superior than those of nano-SiC doping¹⁴ for the optimum content. Actually in the MgB_{2-x}C_x system, substitution of carbon at boron site results in intrinsic flux pinning along with the extrinsic pinning by excess carbon, not going at boron site but present at grain boundary. Thus, it enhances the critical parameters both ways and results in superior results than through other dopants.¹³⁻¹⁵ Substantial increment is noticed in the $H_{c2}(0)$ value for the nanocarbon doped samples as compared to pristine MgB₂ on applying suitable theoretical model. The quantitative description is given in Sec. III and is also compared with the literature. Thus, hereby, we revisit our earlier studied MgB_{2-x}C_x series¹⁶ with high field magnetotransport study up to 140 kOe applied

a) Author to whom correspondence should be addressed. FAX: 0091-11-25626938. Tel.: 0091-11-25748709. Electronic mail: awana@mail.nplindia.ernet.in. URL: www.freewebs.com/vpsawana/.

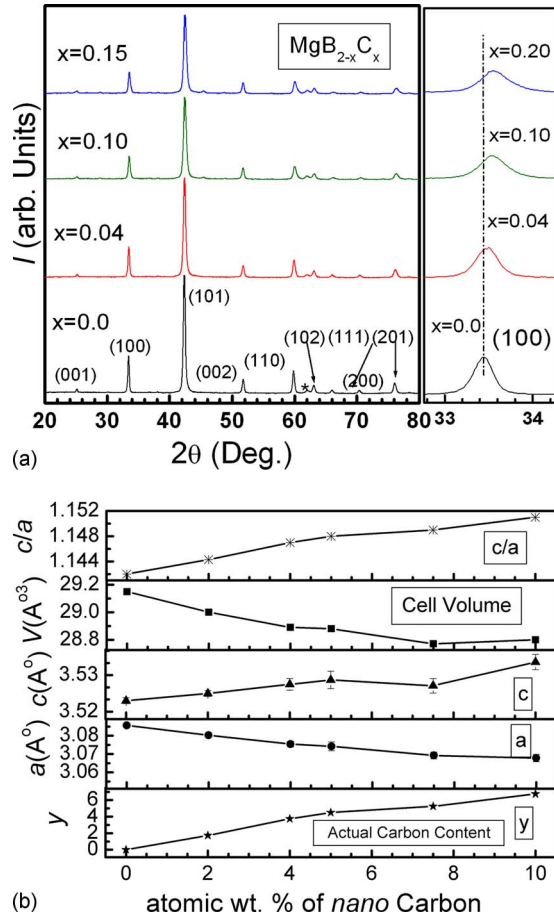


FIG. 1. (Color online) (a). X-ray diffraction patterns for the $\text{MgB}_{2-x}\text{C}_x$ series ($x=0.0, 0.04, 0.10$, and 0.15). (b). Variation in lattice parameters, cell volume, and exact carbon content for $\text{MgB}_{2-x}\text{C}_x$ series ($x=0.0-0.20$).

field in this article. The transition temperature is still 5.80 K for the MgB_2 sample, while the same are 12.80 and 11.30 K for the $x=0.10$ and $x=0.15$ samples at 140 kOe. Thus, the $H_{c2}(0)$ cannot be obtained experimentally. To determine $H_{c2}(0)$ value, we applied different theoretical models such as WHH formula and GL theory. Magnetization measurements confirm the enhanced critical parameters for carbon doped samples in comparison to pure MgB_2 sample.

II. EXPERIMENTAL

The polycrystalline $\text{MgB}_{2-x}\text{C}_x$ samples were synthesized by solid-state reaction route in the argon environment. The detailed procedure of synthesis of samples is given in Ref.

16. X-ray diffraction patterns were taken on Rigaku-Miniflex-Ultima desktop diffractometer. Rietveld refinement was carried out using the software FULLPROOF-2007. Resistivity measurements were made on bar shaped samples using four-probe technique under the constant applied field on Quantum Design PPMS. Magnetization measurements were also carried out on Quantum Design PPMS equipped with vibrating sample magnetometer (VSM) attachment.

III. RESULTS AND DISCUSSIONS

The x-ray diffraction patterns for the pristine and some of the nanocarbon doped samples are shown in Fig. 1(a). Phase purity is checked by Rietveld refinement; all Bragg peaks are obtained at exact position with appropriate intensity. A small intensity extra phase MgO peak is also noticed in the pattern of MgB_2 , which is marked by the symbol “*” in the figure. The nanocarbon doped samples have the similar patterns with the shifted peaks according to the changed lattice parameters. The (100) peak shifts toward higher angle side, shown in the inset of Fig. 1(a), indicating the continuous decrease in the a parameter. Rietveld refinement is done on all the samples and the so obtained lattice parameters are tabulated in Table I. a parameter decreases continuously as expected with the increase in nanocarbon content in $\text{MgB}_{2-x}\text{C}_x$ samples, while c parameter does not change much. For pure MgB_2 sample, the lattice parameter a is found to be 3.0857(8) Å and the same decreases to 3.0678(20) Å for the highest nanocarbon doped sample. The variation in lattice parameters, c/a value, and cell volume with the increasing nanocarbon content is shown in Fig. 1(b). Error bars for the lattice parameters a and c are also drawn as obtained from Rietveld refinement. Cell volume and lattice parameter a both decrease with an increase in x (nanocarbon content in $\text{MgB}_{2-x}\text{C}_x$) while c/a value increases with the increasing nanocarbon amount because of decreasing a parameter and almost constant c value. The continuous monotonic change in lattice parameters confirms the substitution of nanocarbon at boron site in MgB_2 matrix but still the exact amount of nanocarbon substituted at boron site is not known. The exact carbon content in $\text{Mg}(\text{B}_{1-y}\text{C}_y)_2$ is evaluated indirectly using the equation $y=7.5 \times \Delta c/a$, where $\Delta c/a$ is the change in c/a value as compared to the pure sample and y is the exact content by atomic wt % of nanocarbon substituted at the boron site.^{17–19} The exact value calculated in this way is found to be quite less than expected. The net maximum substitution level is just 6% by atomic

TABLE I. Lattice parameters, c/a values, and cell volume are categorized for $\text{MgB}_{2-x}\text{C}_x$ samples ($x=0.0, 0.02, 0.04, 0.06, 0.08, 0.10, 0.15$, and 0.20).

Sample	Atomic wt % of carbon	a (Å)	c (Å)	Volume (Å ³)	c/a	Actual wt % of carbon
MgB_2	0	3.0857(8)	3.5230(8)	29.15	1.142	0
$\text{MgB}_{1.96}\text{C}_{0.04}$	2	3.0803(7)	3.5250(8)	29.0	1.144	1.73
$\text{MgB}_{1.92}\text{C}_{0.08}$	4	3.0754(16)	3.5275(16)	28.89	1.147	3.75
$\text{MgB}_{1.90}\text{C}_{0.10}$	5	3.0742(24)	3.5287(24)	28.88	1.148	4.5
$\text{MgB}_{1.85}\text{C}_{0.15}$	7.5	3.0692(19)	3.5271(20)	28.77	1.149	5.25
$\text{MgB}_{1.80}\text{C}_{0.20}$	10	3.0678(20)	3.5336(21)	28.80	1.151	6.75

weight while the samples were prepared up to 10% by atomic weight. The $x=0.2$, i.e., $\text{MgB}_{1.80}\text{C}_{0.20}$ or $\text{Mg}(\text{B}_{0.90}\text{C}_{0.10})_2$ corresponds to $\text{Mg}(\text{B}_{0.94}\text{C}_{0.06})_2$ or 6% by atomic weight, instead of nominal 10 wt %. The remaining nanocarbon stays at the grain boundary or at interstitial site and acts as a pinning center and hence helps in enhancing the H_{c2} , H_{irr} , and $J_c(H)$ values. This is called the extrinsic pinning. The net carbon, which exactly goes at the boron site, creates disorder in the sigma band and causes intrinsic pinning to enhance the critical parameters. Thus, substitution by carbon at boron site causes extrinsic/intrinsic pinning through additions/substitution and enhances the superconducting performance of MgB_2 both ways. The variation in the exact carbon content, y with the experimentally doped nanocarbon content by atomic wt %, is also plotted at the bottom layer of Fig. 1(b). The observed variation in the lattice parameters is in confirmation with the earlier reports, pertaining to carbon doping in MgB_2 .^{17,20}

Figures 2(a)–2(c) depict the variation in resistivity with temperature in the transition zone at different field values varying from 0 to 140 kOe for the undoped, $x=0.10$, and $x=0.20$ samples, respectively. Here, we note that the transition is very sharp at zero field for all the samples but the transition width increases with the increase in field value. At low fields, behavior of pure sample is better than that of doped samples. The transition temperature $T_c(\rho=0)$ is 37.75 K for pure MgB_2 while it decreases with the boron site nanocarbon substitution to 35.95 and 34.95 K for $x=0.10$ and 0.20 samples, respectively, at zero field value. With increment in applied field, the resistance curves shift toward lower temperature side both for doped and undoped samples, but we can clearly see that relative shift is much lesser in the case of doped sample curves than the pure one. Transition temperature for pure MgB_2 sample is only 5.80 K under 140 kOe field, while is increased to 12.80 and 11.30 K for $x=0.10$ and $x=0.15$ samples, respectively. Thus, addition of nanocarbon clearly improves the superconducting performance of bulk MgB_2 sample at elevated fields. It simply implies that the critical field increases with the nanocarbon doping in MgB_2 . The transition temperatures $T_c(\rho=0)$ for all the synthesized samples at fields varying from 0 to 140 kOe are given in Table II. Moreover, the normal state resistivity (ρ_N) also increases from $35 \mu\Omega \text{ cm}$ for pure MgB_2 to about $140 \mu\Omega \text{ cm}$ for $x=0.10$ and 0.20 samples [see Fig. 2(a)–2(c)]. The increased value of normal state resistivity with nanocarbon doping indicates toward the increased impurity scattering. The value of upper critical field especially $H_{c2}(0)$ is found to depend directly on ρ_N .¹⁰ Thus, this observation is also in confirmation to the enhanced H_{c2} for nanocarbon doped samples. The variation in normalized resistivity (ρ_T/ρ_{40}) with temperature for undoped and some of the nanocarbon doped samples is shown in Fig. 2(d). According to the definition of residual resistivity ratio, RRR value ($=\rho_{300}/\rho_{40}$), the value of normalized resistivity (ρ_T/ρ_{40}) at the end point of curves in Fig. 2(d), i.e., at 300 K, directly corresponds to the RRR value for a particular sample. The RRR value is also plotted with the varying carbon content in the inset of Fig. 2(d). Pure sample is found to have highest value of RRR($=3.6$) among the whole series of $\text{MgB}_{2-x}\text{C}_x$

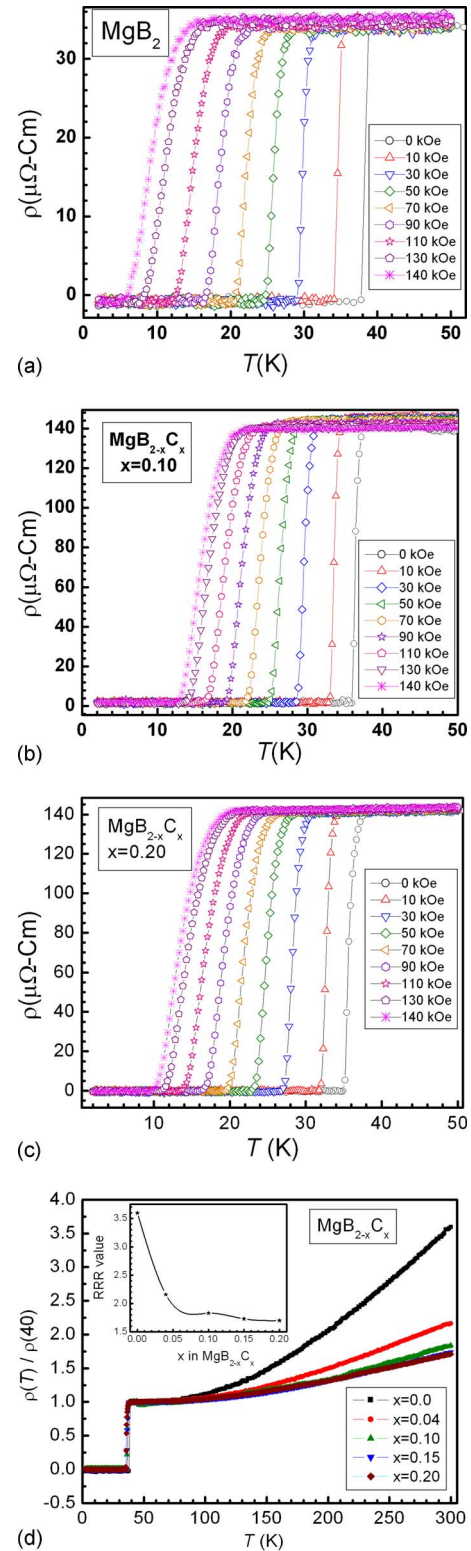


FIG. 2. (Color online) Resistivity vs temperature plot at different field values varying from 0–140 kOe for (a) pure MgB_2 , (b) $\text{MgB}_{2-x}\text{C}_x$, $x=0.10$, and (c) $\text{MgB}_{2-x}\text{C}_x$, $x=0.20$. (d) Variation in normalized resistivity (ρ_T/ρ_{40}) with temperature is shown for $\text{MgB}_{2-x}\text{C}_x$ series ($x=0.0, 0.04, 0.10, 0.15, \text{ and } 0.20$). The RRR values are plotted with the carbon content in the inset.

samples. With an increase in nanocarbon content, the RRR value has a monotonic decrease and the least value of 1.70 is obtained for the highest doped $x=0.20$ sample. It decreases very sharply in the beginning up to $x=0.04$ sample and after that rate of decrease in RRR value with respect to the in-

TABLE II. Transition temperature (T_c at $R=0$) at different field values (0–14 T) for $\text{MgB}_{2-x}\text{C}_x$ samples.

Sr. No.	x in $\text{MgB}_{2-x}\text{C}_x$	T_c $H=0$ kOe	T_c $H=10$ kOe	T_c $H=30$ kOe	T_c $H=50$ kOe	T_c $H=70$ kOe	T_c $H=90$ kOe	T_c 110 kOe	T_c 130 kOe	T_c 140 kOe
1	0.0	37.75	34.10	29.03	24.55	20.55	16.54	12.30	8.06	5.80
2	0.04	36.79	33.60	29.04	25.05	22.06	18.55	15.55	12.30	10.55
3	0.08	36.19	32.80	27.80	24.04	20.29	17.30	14.04	11.30	10.05
4	0.10	35.95	32.80	28.30	24.79	21.55	19.04	15.80	13.80	12.80
5	0.15	35.19	32.55	27.79	23.80	20.30	17.54	15.05	12.54	11.30
6	0.20	34.69	31.55	26.82	22.81	19.30	16.04	13.30	10.79	9.29

creasing nanocarbon content decreases. The nanocarbon doping enhances the electron scattering in the doped sample and hence results in the decreased value of RRR. The above trend of change in RRR values of our samples is in confirmation with the literature.^{17,18}

The critical field is determined for all the samples using the criterion that $H_{c2}=H$ at which $\rho=90\%\rho_N$ and ρ_N is the normal resistivity or resistivity at about 40 K. The transition temperature with this criterion of $\rho=90\%\rho_N$ instead of $\rho=0$ are also determined for all the samples and are tabulated in Table III. The value of applied field in a column directly corresponds to the H_{c2} value at the temperature given below in that column for corresponding samples. The variation in critical fields with temperature is shown in Fig. 3 for undoped as well as the nanocarbon doped samples. At lower fields of less than 30 kOe, all samples have competing value of H_{c2} but as the field increases, performance of nanocarbon doped samples become far better than the undoped sample. As the carbon content increases, H_{c2} also rises and the performance of $x=0.08, 0.10,$ and 0.15 at higher fields is found to be competitive and best among this batch of samples. The other samples with $0.08 > x > 0.15$ have slightly inferior performance but still it is quite better than the pure sample. This is because for the samples with $x < 0.08$, the optimum level of nanocarbon substitution is not reached yet and for $x > 0.15$, the nanocarbon may not go at the boron site and remains at the grain boundary. This can also induce grain boundary pinning but after a limit agglomeration of nanocarbon particles take place so that the size of agglomerated clusters no longer remain of the range of coherence length of MgB_2 and become unable to pin the vortices. At 18.5 K the critical field of MgB_2 is near about 100 kOe while the same is increased to 140 kOe for $x=0.10$ nanocarbon doped sample and lies in the range 120–140 kOe for other nanocarbon doped samples. But since the measurements are done only up to 140 kOe and the temperature is still 18.5K for the

$x=0.10$ sample, it is not possible to find H_{c2} at lower temperatures experimentally. Thus, some theoretical models are needed to be applied to see the behavior of upper critical field at low temperatures.

The simplest model to determine the upper critical field value at 0 K, i.e., $H_{c2}(0)$ is the WHH formulation.

According to the WHH formula,

$$H_{c2}(0) = 0.69T_c(dH_{c2}/dT)_{at T=T_c}. \quad (1)$$

For $x=0.10$ sample, $H_{c2}(0)$ is just equal to 95 kOe by above formula which is not at all acceptable because the critical field of 140 kOe is already achieved at a temperature of 18.5 K. Thus, it is not possible that critical field decreases with a decrease in temperature. Thus, hereby we discard this formula for our system because it underestimates the $H_{c2}(0)$ value. This is also discussed by Huang *et al.*¹² that $H_{c2}(0)$ value calculated by WHH formula is lesser than the real value by a factor of 5 or 6.

Another model applied for H_{c2} determination is GL theory. The GL equation²¹ in two band superconductors such as MgB_2 for temperature dependence of H_{c2} is given by

$$H_{c2}(T) = [H_{c2}(0)\theta^{1+\alpha}]/[1 - (1 + \alpha)\omega + \omega^2 + m\omega^3], \quad (2)$$

where $\theta=1-T/T_c$ and $\omega=(1-\theta)\theta^{1+\alpha}$. The fitting of H_{c2} versus T data is done according to Eq. (2). Both the experimental and fitted curves for H_{c2} are shown in Fig. 4. The fitted curves are in solid line while the experimental data points are shown by symbol. The theoretical curve fits very well with the experimental data up to the limit we carry out the measurements. Thus, the H_{c2} line is drawn theoretically according to Eq. (2). From the fitting, we can clearly see that, initially, the behavior of H_{c2} with T is linear near T_c and extends up to a temperature of 10 K and after that it saturates in the range 3–10 K. Below 3 K the H_{c2} line has negative curvature. The $H_{c2}(0)$ for $x=0.15$ sample is found to be

TABLE III. Transition temperature (T_c at $R=90\%R_{40}$) to determine H_{c2} at different field values (0–14 T) for $\text{MgB}_{2-x}\text{C}_x$ samples.

Sr. No.	x in $\text{MgB}_{2-x}\text{C}_x$	T_c $H=0$ kOe	T_c $H=10$ kOe	T_c $H=30$ kOe	T_c $H=50$ kOe	T_c $H=70$ kOe	T_c $H=90$ kOe	T_c 110 kOe	T_c 130 kOe	T_c 140 kOe
1	0.0	38.84	35.10	30.73	27.28	24.01	20.58	17.60	14.18	12.47
2	0.04	37.72	34.79	30.88	27.81	25.30	22.63	20.28	18.02	16.77
3	0.08	37.19	34.25	30.48	27.63	25.20	23.02	20.91	18.99	17.98
4	0.10	37.04	34.11	30.52	27.93	25.52	23.42	21.50	19.56	18.57
5	0.15	37.10	33.97	30.29	27.62	25.05	22.82	20.76	18.73	17.77
6	0.20	36.64	33.43	29.53	26.87	24.37	22.0	20.05	17.92	17.00

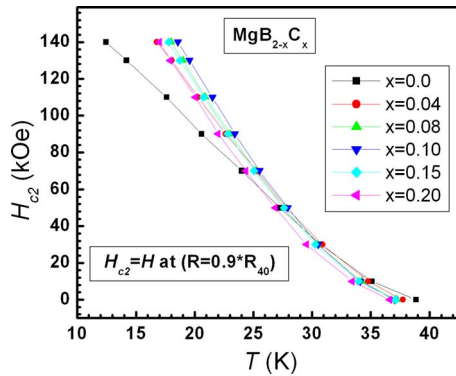


FIG. 3. (Color online) H_{c2} vs temperature plots for $\text{MgB}_{2-x}\text{C}_x$ ($x=0.0-0.20$) samples.

about 300 kOe while the same is just nearly 160 kOe for the pure MgB_2 sample. All the nanocarbon doped samples have $H_{c2}(0)$ values higher than the undoped sample. Thus, GL theory also confirms the enhancement of H_{c2} with carbon doping in MgB_2 and determines the $H_{c2}(0)$ value. The exact values of $H_{c2}(0)$ for all samples is written in the inset of Fig. 4. The $H_{c2}(0)$ value determined by us matches well with Askerzade *et al.*²¹ for the undoped sample and in addition we have applied the same on nanocarbon doped samples and achieved a considerable high value of 300 kOe. The $H_{c2}(0)$ values determined for the nanocarbon doped samples are also in confirmation with other reports in which high field measurements by pulsed magnetic field are carried out.²²

There is one more model known as Gurevich theoretical model for two band superconductors.¹¹ It takes into account the impact of both bands on the critical parameters. If we would have applied this model, the $H_{c2}(0)$ value had been obtained as high as 400 kOe (Refs. 12 and 23) in the case of bulk and 500 kOe in the case of thin films.^{10,24} This actually corresponds to the real situation in the case of MgB_2 because the negative curvature in H_{c2} line near $T=0$ K according to GL equation is not expected. Thus, this theory proves very good for high temperature roughly above 5 K. But below 5 K, the Gurevich model seems to be the best choice. Such a high value of above 400 kOe is really appreciable which proves this material to be a merit candidate for practical applications against Nb based superconductors and HTSC materials.

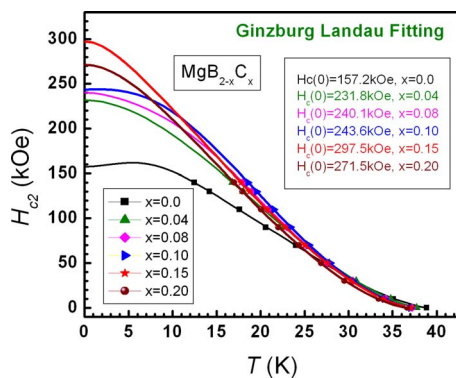


FIG. 4. (Color online) Theoretically fitted curves for H_{c2} vs temperature plots for $\text{MgB}_{2-x}\text{C}_x$ ($x=0.0-0.20$).

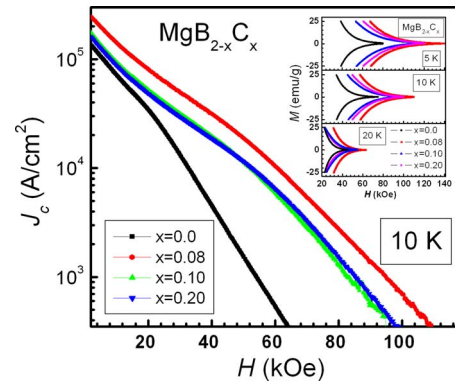


FIG. 5. (Color online) $J_c(H)$ plots for $\text{MgB}_{2-x}\text{C}_x$ samples ($x=0.08, 0.10,$ and 0.20) along with pristine MgB_2 at 10 K in the main panel while the inset shows the magnetization loop $M(H)$ at 5, 10, and 20 K for $\text{MgB}_{2-x}\text{C}_x$ samples ($x=0.0, 0.08, 0.10,$ and 0.20) up to 120 kOe field.

The magnetization hysteresis loop, i.e., magnetization versus applied field curves, are shown for doped and undoped samples in both increasing and decreasing field directions at 5, 10, and 20 K in the inset of Fig. 5. The $M-H$ loop for pure sample closes much before than the doped sample at each temperature, which clearly demonstrates the enhanced value of irreversibility field (H_{irr}). At 5 K, the loop closes nearly at about 80 kOe for the pure sample but is still open at 137 kOe for the nanocarbon doped $x=0.08$ sample. All doped samples have better performance than the undoped samples. To have a clear idea, H_{irr} (irreversibility field) are estimated for all samples at 5, 10, and 20 K from their respective magnetization loops. H_{irr} is taken as the applied field value at which the magnetization loop almost closes with a criterion of giving critical current density value of the order of 10^2 A/cm². For pristine sample, the H_{irr} values are 45, 74, and 80 kOe at 20, 10, and 5 K, respectively, whereas it is increased to 63, 110, and 137 kOe for the $x=0.08$ sample at the same temperatures. These values are slightly higher than those reported earlier by Solatnian *et al.*²⁵ The increased values of H_{irr} confirm the flux pinning by added nanocarbon particles.

The critical current density is calculated from the magnetization hysteresis loops using Bean's critical model. The variation in J_c with applied fields is shown in Fig. 5 for doped and undoped samples at 10 K. All samples have J_c of the order of more than 10^5 A/cm² at low field values. As the field increases, J_c values decrease very rapidly for the pure sample and becomes of the order of 10^2 A/cm² at a field of 60 kOe at 10 K while it is still of the order of 10^4 for the $x=0.08$ sample. Quantitatively, J_c is about 1.04×10^4 A/cm² at 60 kOe and 10 K for $x=0.08$ nanocarbon doped sample, whereas it is 5.4×10^2 A/cm² for pure sample at the same field and temperature values. More specifically, J_c of this sample is 21 times higher than the pure sample at 60 kOe and 10 K. The critical current density value is enhanced similarly at other temperatures also (say, 5 and 20 K) in the case of nanocarbon doped samples. The ensuing pinning plots and the $J_c(H)$ performance of all samples at various temperatures are shown in Ref. 16 by some of us. The observed values of H_{c2} , H_{irr} , and $J_c(H)$ are competitive or slightly better than those being reported yet.²⁶⁻²⁹

IV. CONCLUSION

The nanocarbon doped $\text{MgB}_{2-x}\text{C}_x$ system is studied for the enhanced critical parameters H_{irr} , $J_c(H)$, and especially the upper critical field H_{c2} . Theoretical models are applied on temperature dependence of upper critical field in order to estimate the critical field at low temperatures. $H_{c2}(0)$ for all the carbon doped samples is found to be higher than the pure MgB_2 sample. The $H_{c2}(0)$ value for pure sample is just 157 kOe which got profoundly enhanced and the highest value of $H_{c2}(0)$ of about 300 kOe is achieved for $x=0.15$ sample. The $H_{c2}(0)$ of about 400 kOe is expected by applying the new two band Gurevich model on this system. Not even the upper critical field but the other parameters such as H_{irr} and $J_c(H)$ are also improved significantly for the carbon doped samples.

ACKNOWLEDGMENTS

The authors from NPL would like to thank Dr. Vikram Kumar (DNPL) for his great interest in present work. M.M. would like to thank the CSIR for the award of Junior Research Fellowship to pursue her Ph.D. degree.

- ¹J. Nagamatsu, N. Nakagawa, T. Muranaka, Y. Zenitani, and J. Akimitsu, *Nature (London)* **410**, 63 (2001).
- ²S. L. Bud'ko, G. Lapertot, C. Petrovic, C. E. Cunningham, N. Anderson, and P. C. Canfield, *Phys. Rev. Lett.* **86**, 1877 (2001).
- ³J. Kortus, I. I. Mazin, K. D. Belashchenko, V. P. Antropov, and L. L. Boyer, *Phys. Rev. Lett.* **86**, 4656 (2001).
- ⁴J. M. An and W. E. Pickett, *Phys. Rev. Lett.* **86**, 4366 (2001).
- ⁵H. Kotegawa, K. Ishida, Y. Kitaoka, T. Muranaka, and J. Akimitsu, *Phys. Rev. Lett.* **87**, 127001 (2001).
- ⁶G. Satta, G. Profeta, F. Bernardini, A. Continenza, and S. Massida, *Phys. Rev. B* **64**, 104507 (2001).
- ⁷K. D. Belashchenko, M. van Schilfgaarde, and V. P. Antropov, *Phys. Rev. B* **64**, 092503 (2001).
- ⁸J. D. Jorgensen, D. G. Hinks, and S. Short, *Phys. Rev. B* **63**, 224522 (2001).
- ⁹S. Margadonna, T. Muranaka, K. Prassides, I. Maurin, K. Brigatti, R. M. Ibberson, M. Irai, M. Takata, and J. Akimitsu, *J. Phys.: Condens. Matter* **13**, L795 (2001).
- ¹⁰V. Ferrando, P. Manfrinetti, D. Marre, M. Putti, I. Sheikin, C. Tarantini, and C. Fedeghini, *Phys. Rev. B* **68**, 094517 (2003).
- ¹¹A. Gurevich, *Phys. Rev. B* **67**, 184515 (2003).
- ¹²X. Huang, W. Mickelson, B. C. Regan, and A. Zettl, *Solid State Commun.* **136**, 278 (2005).
- ¹³J. H. Kim, S. X. Dou, M. S. A. Hossain, X. Xu, X. L. Wang, D. Q. Shi, T. Nakane, and H. Kumakura, *Supercond. Sci. Technol.* **20**, 715 (2007).
- ¹⁴A. Vajpayee, V. P. S. Awana, G. L. Bhalla, and H. Kishan, *Nanotechnology* **19**, 125708 (2008).
- ¹⁵A. Vajpayee, V. P. S. Awana, H. Kishan, A. V. Narlikar, G. L. Bhalla, X. L. Wang, *J. Appl. Phys.* **103**, 07C708 (2008).
- ¹⁶M. Mudgel, V. P. S. Awana, G. L. Bhalla, and H. Kishan, *Solid State Commun.* **146**, 330 (2008).
- ¹⁷M. Avdeev, J. D. Jorgensen, R. A. Ribeiro, S. L. Bud'ko, and P. C. Canfield, *Physica C* **387**, 301 (2003).
- ¹⁸A. Bharathi, S. Jemima Balaselvi, S. Kalavathi, G. L. N. Reddy, V. Sankara Sastry, Y. Hariharan, and T. S. Radhakrishnan, *Physica C* **370**, 211 (2002).
- ¹⁹W. K. Yeoh and S. X. Dou, *Physica C* **456**, 170 (2007).
- ²⁰T. Takenobu, T. Ito, D. H. Chi, K. Prassides, and Y. Iwasa, *Phys. Rev. B* **64**, 134513 (2001).
- ²¹I. N. Askerzade, A. Gencer, and N. Guclu, *Supercond. Sci. Technol.* **15**, L13 (2002).
- ²²R. H. T. Wilke, S. L. Budko, P. C. Canfield, and D. K. Finnemore, *Phys. Rev. Lett.* **92**, 217003 (2004).
- ²³S. Noguchi, A. Kuribayashi, T. Oba, H. Iriuda, Y. Harada, M. Yoshizawa, and T. Ishida, *Physica C* **463–465**, 216 (2007).
- ²⁴V. Braccini, A. Gurevich, J. E. Giencke, M. C. Jewell, C. B. Eom, and D. C. Larbalestier, *Phys. Rev. B* **71**, 012504 (2005).
- ²⁵S. Solatanian, J. Horvat, X. L. Wang, P. Munroc, and S. X. Dou, *Physica C* **390**, 185 (2003).
- ²⁶Z. H. Cheng, B. Shen, J. Sheng, S. Y. Zhang, T. Y. Zhao, and H. W. Zhao, *J. Appl. Phys.* **91**, 7125 (2002).
- ²⁷W. K. Yeoh, J. H. Kim, J. Horvat, X. Xu, M. J. Qin, S. X. Dou, C. H. Jiang, T. Nakane, H. Kumakura, and P. Munroe, *Supercond. Sci. Technol.* **19**, 596 (2006).
- ²⁸M. Herrmann, W. Habler, C. Mickel, W. Gruner, B. Holzapfel, and L. Schultz, *Supercond. Sci. Technol.* **20**, 1108 (2007).
- ²⁹W. K. Yeoh, J. H. Kim, J. Horvat, X. Xu, and S. X. Dou, *Physica C* **460–462**, 568 (2007).